RSC Advances

PAPER

View Article Online
View Journal | View Issue

Cite this: *RSC Adv.*, 2017, **7**, 11101

Optimization of peak current of poly(3,4-ethylenedioxythiophene)/multi-walled carbon nanotube using response surface methodology/central composite design

Nurul Ain A. Talib,[ab] Faridah Salam,[c] Nor Azah Yusof,[ab] Shahrul Ainliah Alang Ahmad[ab] and Yusran Sulaiman*[ab]

Received 1st November 2016
Accepted 24th January 2017

DOI: 10.1039/c6ra26135c

rsc.li/rsc-advances

Modification of electrode surface with poly(3,4-ethylenedioxythiophene)/multi-walled carbon nanotube (PEDOT/MWCNT) composite prepared by electrodeposition technique was reported in this study. The optimization of peak current response of PEDOT/MWCNT was performed by utilizing the combination of response surface methodology and central composite design (RSM/CCD). The effect of each variable and the interaction between three variables *i.e.* the concentration of MWCNT, electrodeposition potential and deposition time were studied and modeled. The statistical analysis showed that the concentration of MWCNT and deposition time have significantly affected the peak current response. A reduced cubic model equation with the coefficient of determination (R^2) value of 0.9973 was developed. The optimized condition predicted by the software was compared with the experiment and resulting in less than 2% error, indicating that this model was reliable and able to predict the peak current response accurately. Additionally, the electrochemical properties, chemical properties and morphology of the optimized modified electrode were characterized by cyclic voltammetry (CV), Fourier transform infrared (FTIR), Raman spectroscopy and field emission scanning electron microscopy (FESEM). The peak current of the optimized PEDOT/MWCNT modified electrode was higher than electrode without MWCNT and the FESEM study demonstrated that the tubular structure of MWCNT was uniformly wrapped by PEDOT. The FTIR and Raman spectra proved that MWCNT was successfully incorporated into PEDOT.

Introduction

Modification of electrode surface may enhance the electrochemical properties of the electrode for various application such as solar cells,[1,2] supercapacitor,[3] organic light-emitting diodes (OLEDs),[4,5] chemical sensors[6,7] and biological sensors.[8–10] Modification of the electrode surface will increase the electrode performance by introducing of interest materials through surface absorption,[11,12] crosslinking agent,[13] covalent bonding,[14] non-covalent bonding[15] or other types of attachment. Therefore, the modification of electrode surface has become critical studies to allow enhancement of electrode properties.

Carbon materials such as carbon nanotube (CNT) is known to have high electrical conductivity, high thermal conductivity and high surface area properties.[16] Generally, CNT can be categorized into single-walled carbon nanotube (SWCNT) and multi-walled carbon nanotube (MWCNT). Incorporation of CNTs with suitable conducting polymers may enhance the electrochemical properties of composites.[17] Conducting polymers play a significant contribution in chemical sensors[18] and biosensors[8,19] by improving the current response. Poly(3,4-ethylenedioxythiophene) (PEDOT) is one of the remarkable conducting polymers due to its ability to exhibit excellent electrochemical stability[17] and has been used widely in the electrode modification. The previous studies have suggested that the synergistic effects of the conducting polymer and the nanotubes composites may improve the surface and electrical properties.[20–22] The unique nanotube structure of CNTs allows this material to bear more electrochemically favorable components.[23] The sp^2 carbons and open ends of nanotube-containing oxygen moieties have enabled CNT to act as a support for the formation of electrochemically functional devices. In biosensor applications, the biological compounds such as protein can be absorbed non-covalently along the lengths of CNT,[24] thus make this material as a suitable constituent in the composites.

[a]*Functional Device Laboratory, Institute of Advanced Technology, Universiti Putra Malaysia, 43400 Serdang, Selangor, Malaysia. E-mail: yusran@upm.edu.my; Fax: +60-389435380; Tel: +60-389466779*

[b]*Department of Chemistry, Faculty of Science, Universiti Putra Malaysia, 43400 Serdang, Selangor, Malaysia*

[c]*Agri-Nanotechnology Programme, Biotechnology and Nanotechnology Research Centre, Malaysian Agricultural Research and Development Institute, 43400 Serdang, Selangor, Malaysia*

In order to prepare highly sensitive sensor platforms, optimization of variables is crucial. As an alternative to traditional optimization by one parameter at a time technique, response surface methodology (RSM) was introduced. This statistical analysis can be used with optional of various experimental designs such as central composite design (CCD),[25] Box–Behnken design[26] and Doehlert design.[27] Advantages of RSM are a low number of experiments to be carried out, individual parameter and the interaction between the analyzed parameters can be studied and the reduction of experimental cost by minimizing the process variation.[28]

In this study, PEDOT/MWCNT modified electrode was prepared by electropolymerization technique. The optimization of the peak current response was performed by RSM/CCD to optimize the concentration of MWCNT, electropolymerization potential and deposition time. The optimized PEDOT/MWCNT composite was characterized by cyclic voltammetry (CV), Fourier transform infrared (FTIR), Raman spectroscopy and field emission scanning electron microscopy (FESEM).

Experimental

Materials

3,4-Ethylenedioxythiophene (EDOT) and multi-walled carbon nanotube (MWCNT) were purchased from Sigma-Aldrich (USA). Potassium hexacyanoferrate ($K_3[Fe(CN)_6]$) and potassium chloride (KCl) were obtained from BDH (England) and Fisher Scientific (UK), respectively. All the chemicals were used as received without further purification. Deionized distilled water (DI water) from Milli-Q ultrapure water system with the resistivity of 18.2 MΩ cm was used as the solvent to prepare all the solutions. Indium tin oxide (ITO) glass was cleaned ultrasonically with acetone, ethanol and DI water for 10 min prior to use.

Functionalization of MWCNT

Functionalization of MWCNT was prepared by adding 0.1 g of MWCNT into a mixture solution (50 mL) of concentrated nitric acid (HNO_3) and concentrated sulphuric acid (H_2SO_4) in 1 : 3 ratio. This mixture was then sonicated for two hours before kept overnight. Functionalized MWCNT was filtered and washed with DI water until pH 7 was obtained followed by dried at 60 °C in the oven.

Preparation of PEDOT/MWCNT composite and determination of peak current

Hybridization of PEDOT/MWCNT was performed by electropolymerization of 0.01 M EDOT in the presence of various concentrations of MWCNT suspension onto ITO glass by chronoamperometry (CA). All the electrochemical measurements were performed using a potentiostat Autolab PGSTATM101 (Metrohm) in a three-electrode system with Ag/AgCl as the reference electrode and platinum coil as the counter electrode. The peak current (I_{pa}) values were determined from the cyclic voltammogram.

Design of experiment and response surface methodology

Important variables on the fabrication of electropolymerized PEDOT/MWCNT onto ITO glass was optimized by using RSM/CCD approach. The concentration of MWCNT (A), electropolymerization potential (B) and deposition time (C) were the independent variables used in this study. The ranges and levels of the chosen variables are tabulated in Table 1 and the output of this model was the peak current response. Three factors with the total of 20 experiment runs were suggested by RSM/CCD using the statistical package (Design Expert 6.0, Stat Ease Inc., MN, USA) as displayed in Table 2. Response surface modeling, statistical analysis, and optimization were conducted with the assistance of this software. Analysis of variance (ANOVA) was used in the analyzing of the output data. The peak current response data from the suggested experiments was expressed by polynomial regression equation to generate a model as shown in eqn (1):

$$Y = \beta_0 + \sum_{i=1}^{k} \beta_i x_i + \sum_{i=1}^{k} \beta_{ii} {x_i}^2 + \sum_{i=1}^{k-1} \sum_{j>i}^{k} \beta_{ij} x_i x_j \qquad (1)$$

where Y represents the predicted responses, β_0 is the constant coefficient, β_i, is the ith linear coefficient, β_{ii} is the quadratic coefficient, β_{ij} is the ijth interaction coefficient, while x_i and x_j represent factors.

Validation of the model and optimization of the peak current response were conducted according to the flowchart in Fig. 1. The optimum values of variables were predicted by the response surface analysis of the combined variables. The constraints in this study were applied to predict the optimum variable conditions that resulting in the highest peak current response by inserting the desired conditions in the Design Expert software. The efficiency of the model was verified by performing the suggested experiments and comparing the output with the predicted results. Residual standard errors (RSE) were used to determine the reliability of the model. The numerical optimization of the response was predicted based on the second order polynomial model.

Characterizations

The optimized PEDOT/MWCNT was characterized by cyclic voltammetry (CV) in 0.01 M $K_3[Fe(CN)_6]$ solution containing

Table 1 Experimental range and level of the respective independent variables

			Actual			Coded level		
Variables/factors	Notation	Unit	Low	Middle	High	Low	Middle	High
Concentration of MWCNT	x_i	mg mL^{-1}	0.010	0.105	0.200	−1	0	1
Electropolymerization potential	x_j	V	1.0	1.2	1.4	−1	0	1
Deposition time	x_k	s	60	210	360	−1	0	1

Table 2 Central composite design (CCD) for electropolymerization of PEDOT/MWCNT using RSM method and experimental peak current response data

Standard	*A*: concentration of CNT (mg mL^{-1})	*B*: electropolymerization potential (V)	*C*: deposition time (s)	Peak current (μA)	
				Experiment	Predicted
1	0.010 (−1)	1.00 (−1)	60 (−1)	186.87	186.86
2	0.200 (1)	1.00 (−1)	60 (−1)	199.19	199.18
3	0.010 (−1)	1.40 (1)	60 (−1)	190.87	190.86
4	0.200 (1)	1.40 (1)	60 (−1)	195.17	195.15
5	0.010 (−1)	1.00 (−1)	360 (1)	197.65	197.64
6	0.200 (1)	1.00 (−1)	360 (1)	194.41	194.39
7	0.010 (−1)	1.40 (1)	360 (1)	192.65	192.64
8	0.200 (1)	1.40 (1)	360 (1)	192.86	192.85
9	0.010 (−1)	1.20 (0)	210 (0)	200.78	200.84
10	0.200 (1)	1.20 (0)	210 (0)	196.68	196.74
11	0.105 (0)	1.00 (−1)	210 (0)	212.77	212.83
12	0.105 (0)	1.40 (1)	210 (0)	216.28	216.34
13	0.105 (0)	1.20 (0)	60 (−1)	217.24	217.30
14	0.105 (0)	1.20 (0)	360 (1)	210.84	210.90
15	0.105 (0)	1.20 (0)	210 (0)	216.96	216.88
16	0.105 (0)	1.20 (0)	210 (0)	215.47	216.88
17	0.105 (0)	1.20 (0)	210 (0)	218.28	216.88
18	0.105 (0)	1.20 (0)	210 (0)	215.76	216.88
19	0.105 (0)	1.20 (0)	210 (0)	218.03	216.88
20	0.105 (0)	1.20 (0)	210 (0)	217.03	216.88

0.1 M KCl in the potential range of 0.2 to 0.6 V at a scan rate of 100 mV s^{-1}. FTIR measurements were carried out using attenuated total reflection (ATR) on Perkin-Elmer spectrophotometer with 16 number of scan and resolution of 4. Raman spectroscopy (Alpha 300R) was performed at an integration time of 5 s, accumulation number of 10 and resolution of 200–300 nm. Field emission scanning electron microscopy (FESEM, JOEL JSM-7600F) was used for surface morphology studies. Samples for FESEM were mounted on the stub followed by coating with platinum. The samples were examined at 5 kV operating voltage with 50 000× magnification. All the characterizations were performed at room temperature.

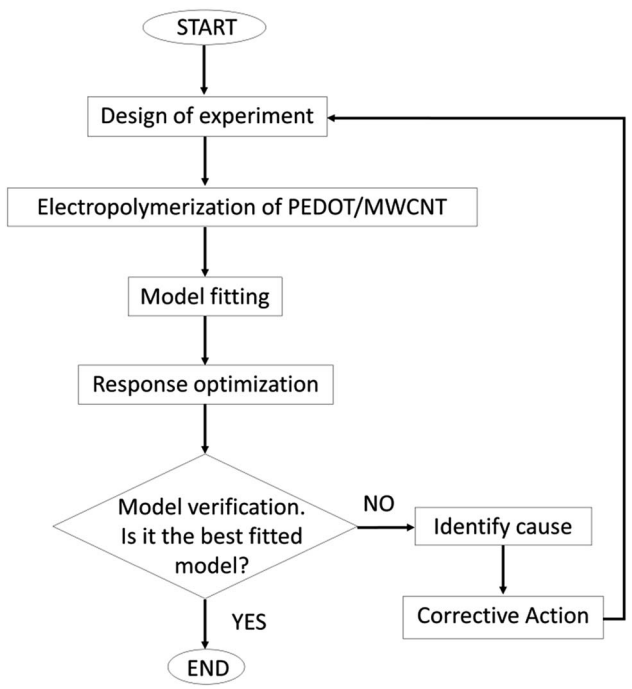

Fig. 1 Experimental flowchart for optimization study.

Results and discussion

Response surface methodology

Model fitting and statistical analysis of the result. The response surface modeling was conducted to establish the optimum conditions (variables) in order to maximize the peak current response of the electropolymerized PEDOT/MWCNT composite. The experimental data in Table 2 was analyzed by Design Expert software and the fitted equation model was constructed. The ANOVA of the peak current response (Table 3) indicates that this model was a highly significant with the prob > *F* value of <0.0001. The prob > *F* less than 0.05 indicates that the model term is significant. The *F*-value of 171.19 also shows the significance of this model. Meanwhile, the *F*-value of 0.02 from the lack of fit implies the insignificant lack of fit which is relative to pure error as the prob > *F* value is 0.8869, which is greater than 0.1000. Not significant lack of fit indicates that this model has good predictability. Since the fit model is desirable, not significant lack of fit is good.

The coefficient of determination of this model is high with the R^2 value of 0.9973 (Table 4). R^2 value closer to linearity indicates good regression. The adjusted R^2 (0.9915) and predicted R^2 (0.9818) values are in reasonable agreement.[29] The value of adequate precision greater than 4 is desirable. Adequate precision measures the signal to noise ratio, which in this case the value of 34.78 is obtained, indicating an adequate ratio. In this

Table 3 ANOVA of the peak current for response surface reduced cubic model

Source	Sum of squares	Degree of freedom	Mean square	*F*-Value	Prob > *F*	
Model	2434.34	13	187.26	171.19	<0.0001	Significant
Residual	6.56	6	1.09			
Lack of fit	0.03	1	0.03	0.02	0.8869	Not significant
Pure error	6.53	5	1.31			
Cor total	2440.90	19				

Table 4 Statistical parameter of the model equation as obtained from ANOVA models for the strength

Types of variables	
Standard deviation (SD)	1.05
Mean	205.29
Coefficient of variation (C.V.)	0.51
Press	44.38
R^2	0.9973
Adjusted R^2	0.9915
Predicted R^2	0.9818
Adequate precision	34.784

study, low coefficient of variation and the standard deviation (SD) values were obtained, implying that this model is good.[30]

The experimental response was modeled as a polynomial equation that represents the effect of experimental independent and dependent variables on the peak current. In this study, there are three variables involved, thus k takes 3. Therefore, the second order polynomial equation becomes eqn (2) with additional cubic interaction effects:

$$Y = \beta_0 + \beta_1 x_1 + \beta_2 x_2 + \beta_3 x_3 + \beta_{11} {x_1}^2 + \beta_{22} {x_2}^2 + \beta_{33} {x_3}^2 + \beta_{12} x_1 x_2 + \beta_{13} x_1 x_3 + \beta_{23} x_2 x_3 + \beta_{112} {x_1}^2 x_2 + \beta_{113} {x_1}^2 x_3 + \beta_{122} x_1 {x_2}^2 + \beta_{123} x_1 x_2 x_3 \quad (2)$$

The intercept (β_0), the main linear (β_1, β_2, β_3), quadratic (β_{11}, β_{22}, β_{33}), cubic (β_{112}, β_{113}, β_{122}, β_{123}) and interaction (β_{12}, β_{13}, β_{23}, β_{112}, β_{113}, β_{122}, β_{123}) effects represent the coefficients in the equation. It is found that the reduced-cubic model fits the experimental data well. The reduced-cubic model equation in coded form based on the data analysis in Table 5 is established in eqn (3):

$$\text{Peak current} = 216.88 - 2.05A + 1.75B - 3.20C - 18.10A^2 - 2.30B^2 - 2.79C^2 - 0.57AB - 2.46AC - 0.82BC - 2.58A^2B + 3.88A^2C + 3.75AB^2 + 1.44ABC \quad (3)$$

Three independent variables *i.e.* the concentration of MWCNT (A), electropolymerization potential (B) and deposition time (C) are represented by coded values ($x_1 = A$, $x_2 = B$ and $x_3 = C$). Model terms of A, C, A^2, B^2, C^2, AC, A^2B, A^2C, AB^2 and ABC are identified as significant model terms with the values of prob > F are lower than 0.0500. Electropolymerization potential (model term B) is an insignificant term in this study, indicating that 1.0 V to 1.4 V potential range for the electropolymerization of PEDOT/MWCNT did not affect the experiment mutually. The model terms AB and BC are identified as insignificant, implying no mutual effect and interaction between the concentration of MWCNT and electropolymerization potential, and also between

Table 5 Coefficient of regression model and their significance

Factor	Coefficient estimate	Degree of freedom	*F* value	Prob > *F*	Standard error	95% confidence interval Low	95% confidence interval High
Intercept	216.88	1			0.36	216.00	217.76
A	−2.05	1	7.68	0.0323[a]	0.74	−3.86	−0.24
B	1.76	1	5.63	0.0553	0.74	−0.05	3.56
C	−3.20	1	18.72	0.0049[a]	0.74	−5.01	−1.39
A^2	−18.10	1	823.45	<0.0001[a]	0.63	−19.64	−16.55
B^2	−2.30	1	13.33	0.0107[a]	0.63	−3.85	−0.76
C^2	−2.79	1	19.54	0.0045[a]	0.63	−4.33	−1.24
AB	−0.57	1	2.39	0.1733	0.37	−1.48	0.33
AC	−2.46	1	44.12	0.0006[a]	0.37	−3.36	−1.55
BC	−0.82	1	4.86	0.0696	0.37	−1.72	0.09
A^2B	−2.58	1	9.71	0.0207[a]	0.83	−4.60	−0.55
A^2C	3.88	1	22.05	0.0033[a]	0.83	1.86	5.91
AB^2	3.75	1	20.54	0.0040[a]	0.83	1.72	5.77
ABC	1.44	1	15.07	0.0082[a]	0.37	0.53	2.34

[a] Significant.

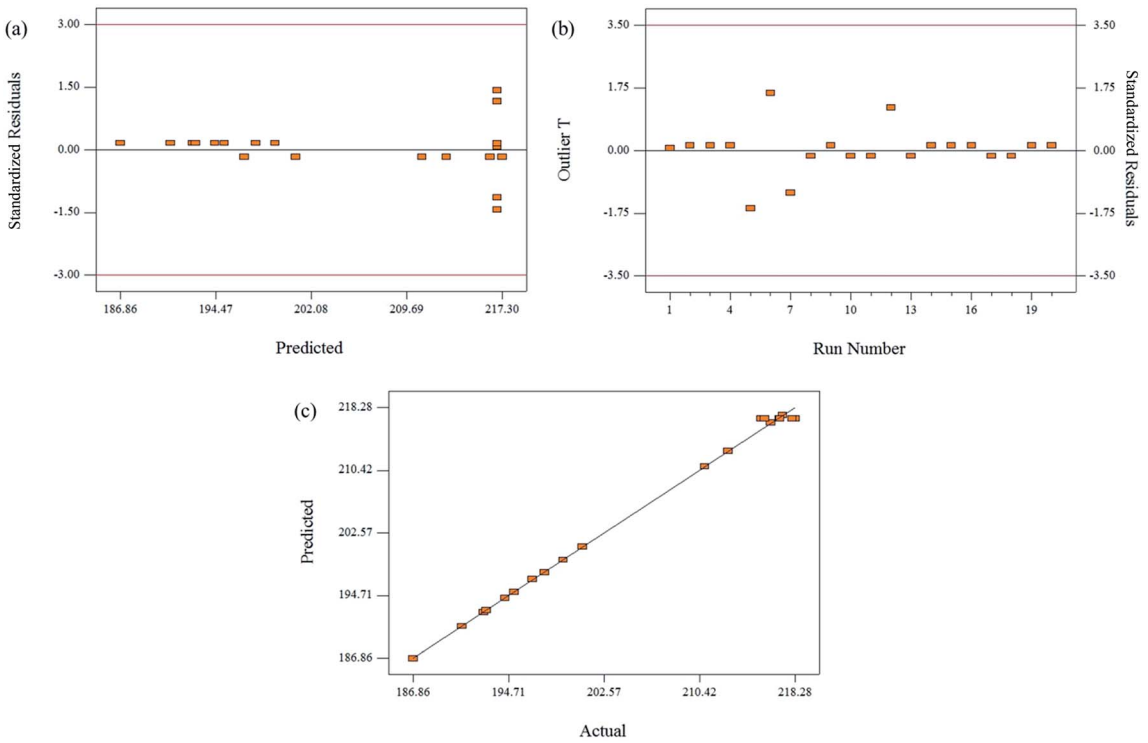

Fig. 2 Plot of (a) residual *versus* predicted response; (b) residual *versus* run and outlier *versus* run; (c) predicted *versus* actual (correlation between the predicted and actual experiment values for the peak current).

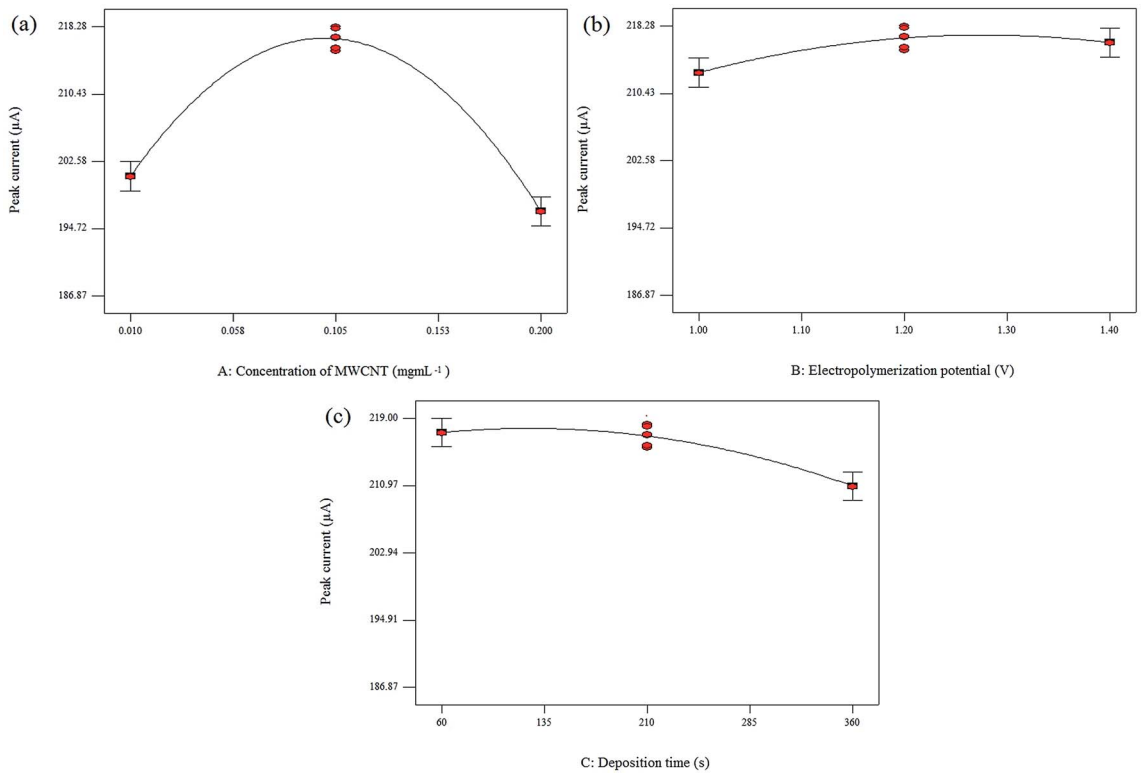

Fig. 3 One factor plot of current response as a function of (a) concentration of MWCNT (electropolymerization potential = 1.20 V; deposition time = 210 s), (b) electropolymerization potential applied (concentration of MWCNT = 0.105 mg mL^{-1}; deposition time = 210 s), and (c) deposition time (concentration of MWCNT = 0.105 mg mL^{-1}; electropolymerization potential = 1.20 V).

electropolymerization potential and deposition time in this study.

Eventhough terms *B*, *AB* and *BC* are insignificant, these terms remain in the model equation to support the hierarchy. The insignificant terms also have a contribution in this model based on the fact that this model design can predict accurate up to 2% RSE according to the model validation. A non-significant term can be remained or removed from the model equation depending on the suitability. However, not removing non-significant terms has become common practice,[31–33] thus it is

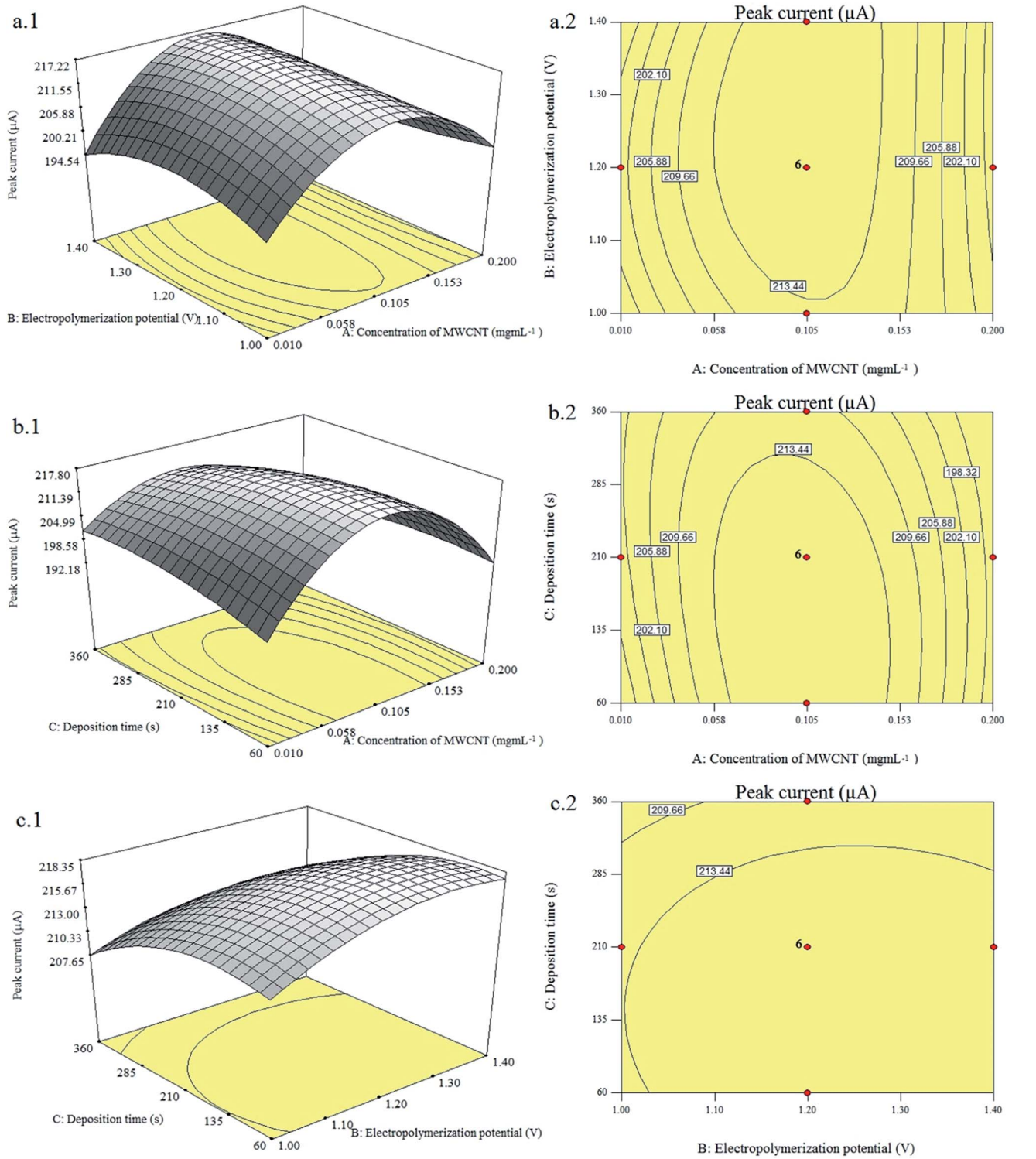

Fig. 4 3D surface and 2D contour plots of peak current as a function of (a) concentration of MWCNT and electropolymerization potential, (b) concentration of MWCNT and deposition time, and (c) electropolymerization potential and deposition time.

not necessary to remove the insignificant terms in this study. The normal cubic equation should include terms A^3, B^3, C^3, AC^2, B^2C and BC^2. However, terms A^3, B^3, C^3, AC^2, B^2C and BC^2 are aliased with terms A, B, C, AB^2, A^2C and AC^2, respectively. Thus, these terms are not required in the equation and were removed resulting the cubic model becomes a reduced-cubic model. Based on the prob > F value, terms A^2B, A^2C, AB^2 and ABC from cubic interactions are significant thus these terms are included in the model.

Diagnostics. The plot of studentized residual *versus* predicted response can be used to determine the adequacy of a model. The plot in Fig. 2a shows uniformly circulated data around the mean point of response variables. This pattern indicates that this model is an adequate model. Randomly scattered data point with no trends in plot studentized residual *versus* run number (Fig. 2b) shows good data distribution. This plot was used to check for any constant error that might occur. Each data distributed nicely inside the limits, implying no constant error detected. This pattern shows no requirement for model transformation or ignoring any data. The plot of outlier *versus* run number (Fig. 2b) shows all points fall within the limits as calculated at 95% confidence level, indicating all the data in this study is acceptable. This plot is used to ensure that all the points fall inside the plus and minus control limits and it can be used to observe any point that is out of the considered range which might also indicate the experimental error. Therefore, all the data in this study is acceptable. The correlation between the predicted and actual experimental values for peak current (Fig. 2c) indicates that highly accurate predicted *versus* actual data plot was obtained by analyzing the linear regression fit. Based on the adequate correlation, the model can accurately represent the experimental data.

Effect of each factor. The value of prob > F for a model term A that represents the concentration of MWCNT is less than 0.0500, indicating a significant term. This statement is in agreement with the one-factor plot in Fig. 3a, in which the peak current response increases as the MWCNT concentration increased from 0.010 mg mL^{-1} to 0.105 mg mL^{-1}. However, the peak current decreases as the MWCNT concentration further increased to 0.200 mg mL^{-1}. Therefore, the best peak current response can be obtained with 0.105 mg mL^{-1} MWCNT based on the individual evaluation of concentration of MWCNT factor. However, only slightly increase of peak current response was observed with the increasing of electropolymerization potential from 1.0 V to 1.4 V (Fig. 3b). Based on this graph, electropolymerization potential between 1.0 V and 1.4 V is not significant, which is in agreement with the insignificant prob > F value calculated from ANOVA. Effect of deposition time plot (Fig. 3c) shows that the peak current response decreases as the deposition time increased from 210 s to 360 s. In comparison with lower deposition time, no apparent change in the peak current was observed between 60 s and 210 s. Therefore, the factor of deposition time is significant when interpreted individually, which is also agreed with the value of prob > F.

Effect of interaction between factors. Fig. 4 shows the three-dimensional (3D) surface and two-dimensional (2D) estimated contour plots of the response surface plots for the peak current response. The other factor remains constant while the interacted factors are shown in this figure. The intense curvature represents the strong interaction between variables, demonstrating that all the studied factors (concentration of MWCNT, electrodeposition potential and deposition time) affect the peak current response of this model.

Validation of model and optimization of peak current. Validation of the model was carried out by performing three set of experiments generated from Design Expert software by comparing the predicted and experimental values. The optimization process was carried out by inserting the desirable criteria as shown in Table 6. The maximum peak current response was set as the main goal, while the other factors are in the studied range. The experiments and the response from the optimization of peak current (Table 7) indicate that all the experiments produce peak current response less than 2% residual standard error (RSE), thus validating the model. Based on the performed experiments, prediction of this model is accurate up to 98%.

Cyclic voltammetry. I_{pa} of the optimized PEDOT/MWCNT composite from RSM was compared with PEDOT modified ITO electrode by cyclic voltammetry (CV) measurements in 1 mM $K_3[Fe(CN)_6]$ mixed with 0.1 M KCl in 0.2 V to 0.6 V potential range. PEDOT, as a conducting polymer allows an acceleration of electron transfer between the electrochemical

Table 6 Constrains applied for optimization

		Limit	
Name	Goal	Lower	Upper
Concentration of MWCNT (mg mL^{-1})	Is in range	0.010	0.200
Electropolymerization potential (V)	Is in range	1.00	1.40
Deposition time (s)	Is in range	60	360
Peak current (μA)	Maximize	186.87	218.28

Table 7 Predicted and observed response values conducted at optimum combination

Number	Concentration of MWCNT (mg mL^{-1})	Electropolymerization potential (V)	Deposition time (s)	Peak current (μA)		RSE (%)
				Predicted	Experiment	
1	0.100	1.31	99.10	218.324	220.25	0.8822
2	0.100	1.33	120.53	218.285	220.76	1.1338
3	0.100	1.29	129.36	218.324	218.16	0.0751

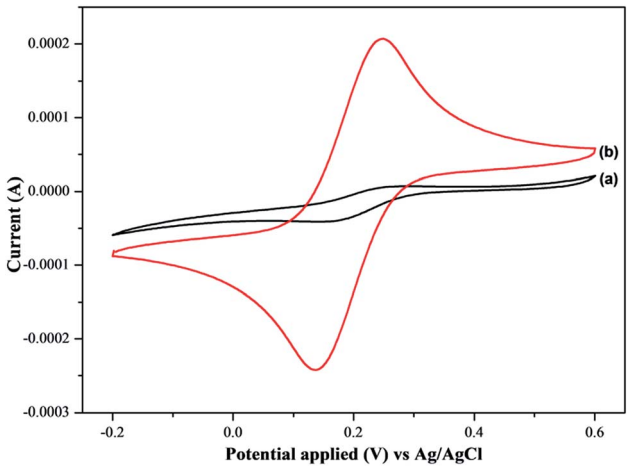

Fig. 5 Cyclic voltammogram of (a) PEDOT and (b) PEDOT/MWCNT.

probe $[Fe(CN)_6]^{3-/4-}$ and the ITO glass as shown in small redox peak in Fig. 5a. Interestingly, by adding MWCNT as a dopant has resulted in an increase of I_{pa} up to 220.25 μA for PEDOT/MWCNT composite (Fig. 5b) in comparison to PEDOT (I_{pa} = 15 μA). This result demonstrates that the synergistic effect[34] between electrocatalytic properties of PEDOT and large surface area of MWCNT has enhanced the electron transfer process.

Fourier transform infrared. In order to understand the changes in the chemical composition of MWCNT before and after functionalization, the FTIR spectra are compared (Fig. 6). Obvious broad and strong peaks in the range of 3550 to 3200 cm^{-1} and 3000 to 2500 cm^{-1} (Fig. 6b) indicate the O–H stretching from hydroxyl and carboxyl group. However, these peaks were not observed in the untreated MWCNT (Fig. 6a), implying that the functionalization of MWCNT was successful after the acid oxidation treatment. Stretching modes of MWCNT backbone are determined by the present of shoulder peaks at 1558 and 1229 cm^{-1} (Fig. 6b) along with a peak at 1721 cm^{-1} which represents the C=O stretching vibration.

Other functional groups such as C=C stretching (quinoidal structure) of the thiophene ring (peaks at 1516 and 1621 cm^{-1}), C–C stretching of the quinoidal structure of the thiophene ring (shoulder peak at 1346 cm^{-1}) and C–O–C stretching in the ethylene dioxy group (1041 cm^{-1}) were also observed. Incorporation of MWCNT into PEDOT composite has resulted in the disappearance of peaks 1721, 1518, 1329 and 1229 cm^{-1} that originated from MWCNT (Fig. 6d). This is due to the MWCNTs were wrapped with the PEDOT,[35] which is also supported by the FESEM image in Fig. 8c. Meanwhile, the other peaks belong to PEDOT can still be observed after the formation of PEDOT/MWCNT composite. Meanwhile, a peak at 1325 cm^{-1} is attributed to the hydroxyl group (O–H) formation from the deformation of the carboxylic group (–COOH) due to acid oxidization of MWCNT. Fig. 6c shows the C–S deformation peaks from PEDOT that determined by the peaks at 984 (shoulder), 834 and 692 cm^{-1}.

Raman spectroscopy. Raman spectra of the untreated MWCNT (Fig. 7a) and functionalized MWCNT (Fig. 7b) are compared based on the intensity of D band and G band (I_D/I_G).

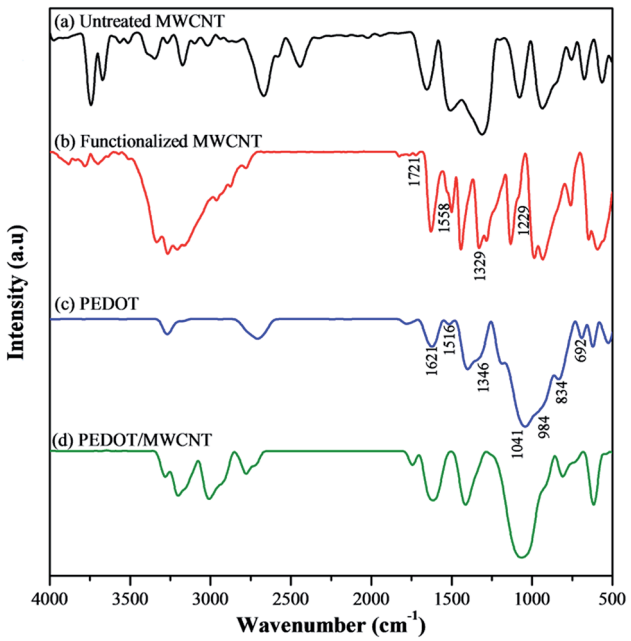

Fig. 6 FTIR spectra of (a) untreated MWCNT, (b) functionalized MWCNT, (c) PEDOT and (d) PEDOT/MWCNT.

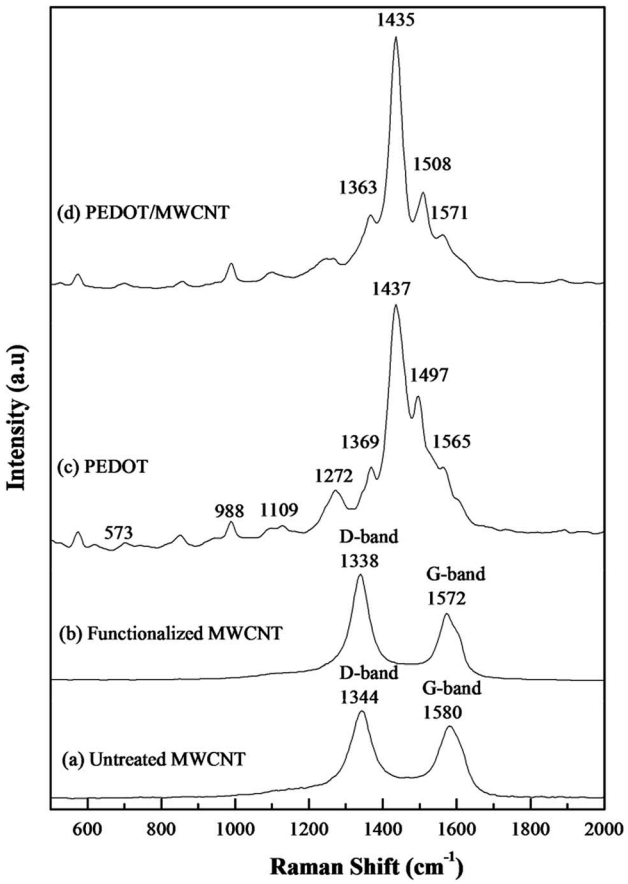

Fig. 7 Raman spectra of (a) untreated MWCNT, (b) functionalized MWCNT, (c) PEDOT and (d) PEDOT/MWCNT.

I_D/I_G value of the untreated MWCNT is determined as 1.21 based on the D band (1344 cm^{-1}) and G band (1580 cm^{-1}). After functionalization with hydroxyl and carboxyl groups, the ratio of I_D/I_G is increased to 1.55. This is in agreement with the fact that the purity of the untreated MWCNT was interrupted and defection has formed. Peaks belong to PEDOT such as oxyethylene group (573 and 988 cm^{-1}), C–C band (1272 cm^{-1}), C–O–C band (1109 cm^{-1}) C_β–C_β band (1369 cm^{-1}), the asymmetric C_α=C_β band (1497 cm^{-1}) and symmetric C_α=C_β band (1437 cm^{-1}) from PEDOT were observed in Fig. 7c. Slightly shifted D band (1363 cm^{-1}) and G band (1571 cm^{-1}) belong to MWCNT along with oxyethylene group, C–C band, C–O–C band, asymmetric C_α=C_β band (at 1508 cm^{-1}) and symmetric C_α=C_β band (1435 cm^{-1}) from PEDOT were observed in the PEDOT/MWCNT composite spectrum (Fig. 7d), indicating that MWCNT was successfully incorporated with PEDOT.

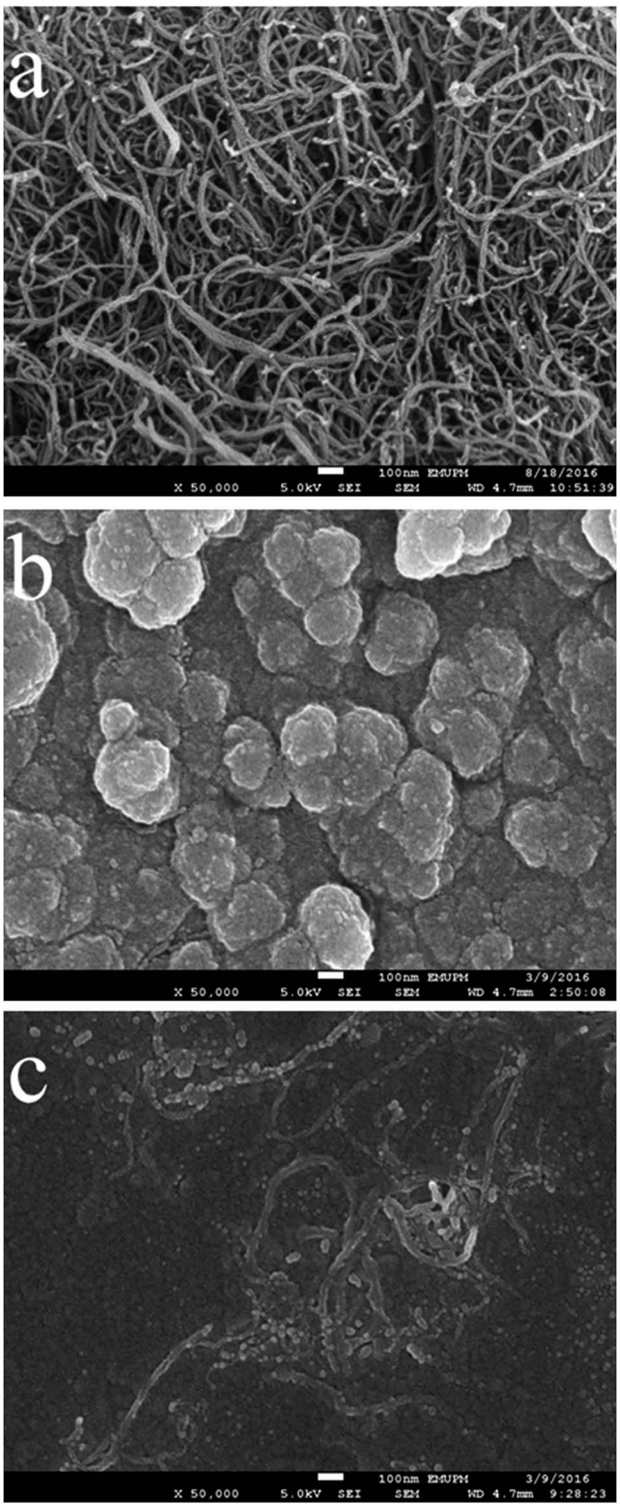

Fig. 8 SEM images of (a) functionalized MWCNT, (b) PEDOT and (c) PEDOT/MWCNT.

Morphology. FESEM was used to study the surface morphology of MWCNT, PEDOT and PEDOT/MWCNT composite. As can be seen, MWCNT exhibits tubular structure (Fig. 8a) and the PEDOT shows nodular structure (Fig. 8b). Electropolymerization of EDOT with MWCNT has resulted in the tubular surface of MWCNT that uniformly wrapped by PEDOT (Fig. 8c). The nodular structure of PEDOT still can be observed after the formation of PEDOT/MWCNT composite. The MWCNTs were efficiently coated by PEDOT through electrostatic attraction.[36] Carboxyl groups from functionalized MWCNT act as the counter ions in this interaction for balancing the positive charge on the PEDOT conducting polymer.

Conclusions

Central composite design/response surface methodology was successfully utilized for the optimization of peak current in the fabrication of PEDOT/MWCNT modified electrode. The effect of three major factors in the fabrication of PEDOT/MWCNT composite was studied and optimized statistically. The concentration of MWCNT and the deposition time were statistically determined as significant terms. Based on response surface optimization, the optimum condition for fabrication of PEDOT/MWCNT composite with maximum peak current was achieved by electrodepositing 0.1 mg mL^{-1} of MWCNT in 0.01 M EDOT at 1.31 V for 99.1 s on the electrode surface. The validation and optimization based on the software prediction have shown that this model can predict with less than 2% error as compared with the experiment, suggesting that this model was reliable and able to predict the peak current response accurately. The optimized PEDOT/MWCNT composite exhibited the tubular structure of MWCNT that uniformly wrapped by PEDOT has significantly improved the electrochemical properties.

Acknowledgements

The authors would like to thank Fundamental Research Grant Scheme (01-01-15-1707FR) for funding this research project and Malaysian Agricultural Research and Development Institute (MARDI) for facilities provided.

References

1 X. Lin, Y. Yang, L. Nian, H. Su, J. Ou, Z. Yuan, F. Xie, W. Hong, D. Yu, M. Zhang, Y. Ma and X. Chen, *Nano Energy*, 2016, **26**, 216–223.

2 H. Seo, M.-K. Son, S. Hashimoto, T. Takasaki, N. Itagaki, K. Koga and M. Shiratani, *Electrochim. Acta*, 2016, **210**, 880–887.
3 N. Hawa, N. Azman, L. H. Ngee and Y. Sulaiman, *Electrochim. Acta*, 2016, **188**, 785–792.
4 R. E. Triambulo and J.-W. Park, *Org. Electron.*, 2016, **28**, 123–134.
5 J. Lee, H. Youn and M. Yang, *Org. Electron.*, 2015, **22**, 81–85.
6 D. Kim, D. Yang, K. Kang, M. A. Lim, Z. Li, C.-O. Park and I. Park, *Sens. Actuators, B*, 2016, **226**, 579–588.
7 W. Chaisriratanakul, W. Bunjongpru, W. Jeamsaksiri, A. Srisuwan, S. Porntheeraphat, E. Chaowicharat, C. Hruanun, A. Poyai, D. Phomyothin and J. Nukeaw, *Surf. Coat. Technol.*, 2016, **306**, 58–62.
8 F. Salam and I. E. Tothill, *Biosens. Bioelectron.*, 2009, **24**, 2630–2636.
9 D. Li, J. Wu, P. Wu, Y. Lin, Y. Sun, R. Zhu, J. Yang and K. Xu, *Sens. Actuators, B*, 2015, **213**, 295–304.
10 Y. Temerk and H. Ibrahim, *Sens. Actuators, B*, 2016, **224**, 868–877.
11 M. Thiruppathi, N. Thiyagarajan, M. Gopinathan and J.-M. Zen, unpublished work.
12 J. Wang, M. Xu, Z. Huangfu, Y. Wang, Y. He, W. Guo and Z. Wang, *Vib. Spectrosc.*, 2016, **85**, 122–127.
13 K. Nakabayashi, D. Noda, T. Takahashi and H. Mori, *Polymer*, 2016, **86**, 56–68.
14 M. Amouzadeh Tabrizi and M. Shamsipur, *Biosens. Bioelectron.*, 2015, **69**, 100–105.
15 J. Zhao, J. Ma, X. Nan and B. Tang, *Org. Electron.*, 2016, **30**, 52–59.
16 R. Isaac and P. K. Praseetha, *Int. J. Electrochem. Sci.*, 2015, **10**, 7303–7319.
17 N. A. Alba, Z. J. Du, K. A. Catt, T. D. Y. Kozai and X. T. Cui, *Biosensors*, 2015, **5**, 618–646.
18 U. Lange, N. V. Roznyatovskaya and V. M. Mirsky, *Anal. Chim. Acta*, 2008, **614**, 1–26.
19 M. Cui, Z. Song, Y. Wu, B. Guo, X. Fan and X. Luo, *Biosens. Bioelectron.*, 2016, **79**, 736–741.
20 M. Ginic-Markovic, J. G. Matisons, R. Cervini, G. P. Simon and P. M. Fredericks, *Chem. Mater.*, 2006, **18**, 6258–6265.
21 M. M. Barsan, M. E. Ghica and C. M. A. Brett, *Anal. Chim. Acta*, 2015, **881**, 1–23.
22 Rajesh, T. Ahuja and D. Kumar, *Sens. Actuators, B*, 2009, **136**, 275–286.
23 L. Su, F. Gao and L. Mao, *Anal. Chem.*, 2006, **78**, 2651–2657.
24 M. M. Barsan, R. C. Carvalho, Y. Zhong, X. Sun and C. M. A. Brett, *Electrochim. Acta*, 2012, **85**, 203–209.
25 T. Rajmohan and K. Palanikumar, *Measurement*, 2013, **46**, 1470–1481.
26 S. L. C. Ferreira, R. E. Bruns, H. S. Ferreira, G. D. Matos, J. M. David, G. C. Brandão, E. G. P. da Silva, L. A. Portugal, P. S. dos Reis, A. S. Souza and W. N. L. dos Santos, *Anal. Chim. Acta*, 2007, **597**, 179–186.
27 T. Lundstedt, E. Seifert, L. Abramo, B. Thelin, Å. Nyström, J. Pettersen and R. Bergman, *Chemom. Intell. Lab. Syst.*, 1998, **42**, 3–40.
28 B. W. Chieng, N. a. Ibrahim and W. M. Z. W. Yunus, *Polym.-Plast. Technol. Eng.*, 2012, **51**, 791–799.
29 K. Mammar and A. Chaker, *Leonardo J. Sci.*, 2013, 84–96.
30 C. García-Gómez, P. Drogui, F. Zaviska, B. Seyhi, P. Gortáres-Moroyoqui, G. Buelna, C. Neira-Sáenz, M. Estrada-alvarado and R. G. Ulloa-Mercado, *J. Electroanal. Chem.*, 2014, **732**, 1–10.
31 S. Agarwal, I. Tyagi, V. K. Gupta, M. Dastkhoon, M. Ghaedi, F. Yousefi and A. Asfaram, *J. Mol. Liq.*, 2016, **219**, 332–340.
32 S. Sugashini and K. M. M. S. Begum, *Clean Technol. Environ. Policy*, 2013, **15**, 293–302.
33 S. E. Ashari, R. Mohamad, A. Ariff, M. Basri and A. B. Salleh, *J. Oleo Sci.*, 2009, **58**, 503–510.
34 R. Mangu, S. Rajaputra and V. P. Singh, *Nanotechnology*, 2011, **22**, 215502.
35 Y. M. Xiao, J. Y. Lin, J. H. Wu, S. Y. Tai and G. T. Yue, *Electrochim. Acta*, 2012, **83**, 221–226.
36 S. Bhandari, M. Deepa, A. K. Srivastava, C. Lal and R. Kant, *Macromol. Rapid Commun.*, 2008, **29**, 1959–1964.